Hybrid Technique Plus Fast Frequency Sweep for the Efficient and Accurate Analysis of Substrate Integrated Waveguide Devices

Angel Belenguer, *Member, IEEE,* Héctor Esteban, *Member, IEEE,* Elena Diaz, *Student Member, IEEE,* Carmen Bachiller, *Graduate Student Member, IEEE,* Joaquin Cascon, Vicente E. Boria, *Senior Member, IEEE*

***Abstract*—In this paper we adapt a novel mode-matching and method of moments hybrid technique to efficiently analyze substrate integrated waveguide based devices. The hybrid technique is formulated in terms of a single equivalent current. This fact is used to include the emergent modal weights, i.e. the scattering parameters, as unknowns of the method of moments system of equations. In this case, it is relatively easy to develop fast frequency sweep schemes that can be used to highly accelerate the solution of an arbitrary device and, as a result, a very efficient technique is obtained. This technique can be applied to the analysis and design of substrate integrated waveguide devices, and it is highly competitive when compared to other method of moments and mode-matching hybrid formulations or when compared to reference commercial software.**

***Index Terms*—EM analysis, mode matching, moment method, modal analysis, substrate integrated waveguides, microwave filters.**

I. Introduction

RECENTLY [1], we presented a novel mode-matching [2] and method of moments [3] hybrid technique that can be used to analyze any device that is fed through canonical waveguides. Generally, these hybrid techniques are formulated by applying the well-known equivalence theorem [4], [5], so that the ports are replaced by a pair of unknown electric and magnetic current densities. A hybrid proposal that uses this pair of currents to achieve the equivalence [6] has been successfully applied to the analysis of substrate integrated waveguide (SIW) [7]–[9] devices. Another recent contribution for the accurate and efficient analysis of SIW circuits is based upon the well-known Boundary Integral - Resonant Mode Expansion (BI-RME) method [10]–[13], which provides the generalized admittance matrix of the SIW circuit in polar form with a reduced number of frequency dependent computations. However, more efforts on increasing the numerical efficiency of these hybrid modal analysis methods can still be developed, specifically by considering other generalized matrix formulations (i.e. the one based on scattering parameters) together with fast frequency sweep schemes.

In [6], the metalized holes, which form the substrate integrated waveguide, are characterized by means of cylindrical emergent spectra. This modal characterization implies an important computational advantage and, since we can use this modal approach in our hybrid formulation, we will apply this idea and try to develop a method as efficient as possible.

In our hybrid formulation we propose a port characterization based on a single electric current density, in opposition to the common strategy based on two equivalent sources, a pair of magnetic and electric current densities. On one hand, this simplification helps in reducing the computational cost of the overall hybrid technique, since the computation of the scattering parameters is much more simple. On the other hand, since the scattering parameters are directly unknowns of the resulting system of equations when our formulation is applied, developing a fast sweep scheme for this kind of problem is relatively easy.

In a first stage, we will test the efficiency and accuracy of a fast frequency sweep developed by means of an asymptotic waveform evaluation (AWE) [14]–[18]. In this technique an approximate response is computed from the analysis of the problem in a single frequency point inside the bandwidth of interest.

Sometimes, the desired bandwidth is so wide that it is not possible to get a good approximation from a single point. A solution to this problem is to use more than one point to develop such an approximation. The main difficulty of this strategy is to find the appropriate points for these partial AWE sub-expansions. In order to find these points, one can use the technique known as complex frequency hopping (CFH) [19], [20]. If we apply this technique, we can ensure that the approximation will be as good as desired provided enough points are considered. The width of the analyzed frequency range will not affect the accuracy of the results, but the cost will be proportionally increased.

In this paper, we will apply both fast sweep approaches and we will discuss their accuracy and efficiency. Finally, we will compare the results to experimental measurements.

II. Problem formulation

Fig. 1 shows that the SIW approximates a rectangular waveguide. It consists on a dielectric thin substrate that is

This work has been supported by Ministerio de Ciencia e Innovación, Spanish Government, under Research Project TEC2007-67630-C03-01, and by the Autonomous Government of Castilla-La Mancha under Research Project PPII10-0047-0220.

A. Belenguer and J. Cascon are with the Departamento de Ingeniería Eléctrica, Electrónica, Automática y Comunicaciones, Escuela Universitaria Politécnica de Cuenca, Universidad de Castilla-La Mancha, Campus Universitario, 16071 Cuenca, Spain (e-mail: angel.belenguer@uclm.es; joaquin.cascon@uclm.es).

H. Esteban, E. Diaz, C. Bachiller and V. E. Boria are with the Departamento de Comunicaciones, Universidad Politécnica de Valencia, 46022 Valencia, Spain (e-mail: hesteban@dcom.upv.es; eldiaca@teleco.upv.es; mabacmar@dcom.upv.es; vboria@dcom.upv.es).

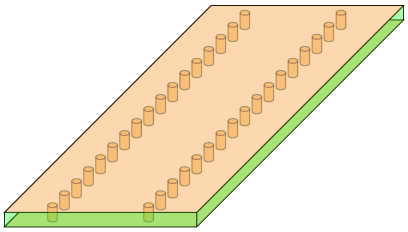

Fig. 1. SIW geometry.

metalized on both faces. These faces act as the upper and lower walls of the waveguide. On the other hand, the side walls of the rectangular waveguide are replaced by a set of small conducting cylinders (via holes) that are placed close enough to each other to approximate the side walls.

Since the cylinders are invariant along the vertical dimension, and considering that no power is leaking out of the SIW, a SIW can be very well approximated by a completely bi-dimensional scattering problem. If we apply this approximation, it will be only necessary to consider the modes of the SIW that correspond to the TE_{m0} modes of the equivalent ideal rectangular waveguide [1], [6], [21], [22].

In order to characterize the cylinders, we will expand the field scattered by each cylinder as a linear superposition of cylindrical modes that emerge from its center, i.e.

$$\vec{E}_i(\underline{c}_i, \vec{\rho}) = \sum_{n=-\infty}^{\infty} \hat{c}_n^{(i)} H_n^{(2)}(k|\vec{\rho} - \vec{\rho}_i|) e^{\jmath n\phi} \hat{y} \tag{1}$$

where, $\vec{E}(\underline{c}_i, \vec{\rho})$ is the field emergent from the i-th cylinder evaluated at $\vec{\rho}$; $H_n^{(2)}$ is the Hankel function of order n; k is the wavenumber; ϕ is the angle that $\vec{\rho}$ forms with the x-axis; $\vec{\rho}_i$ is the position of the center of the i-th cylinder; $\hat{y}$ is a unitary vector perpendicular to the metallic walls that limit the dielectric substrate; $\hat{c}_n^{(i)}$ is the weight associated to the n-th mode emerging from the i-th cylinder; and $\underline{c}_i$ is a vector that contains all the modal weights belonging to the i-th cylinder.

For computational reasons, we cannot consider infinite emergent spectra. Therefore, we necessarily have to truncate the series of (1). In order to truncate the series, we have applied a truncation criteria, which depends on the radius of the characterized cylinder, r_i. Specifically, we have determined the highest order mode to be considered, N_i, applying the following expression,

$$N_i = \max\left\{3, \text{ceil}\left(4\pi r_i/\lambda\right)\right\} \tag{2}$$

where ceil(A) rounds the elements of A to the nearest integer greater than or equal to A. With this equation we ensure that N_i is at least 3 no matter how small the cylinder is, thus ensuring a good accuracy. We have fixed a minimum value in order to prevent a small cylinder from being characterized by an excessively low number of modes.

Finally, the electric field that the i-th cylinder emits can be computed,

$$\vec{E}_i(\underline{c}_i, \vec{\rho}) = \sum_{n=-N_i}^{N_i} \hat{c}_n^{(i)} H_n^{(2)}(k|\vec{\rho} - \vec{\rho}_i|) e^{\jmath n\phi} \hat{y} \tag{3}$$

so that we will have to determine $2N_i + 1$ different modal weights for every considered cylinder.

Hankel functions diverge when its argument is small and its order progressively increases and becomes larger than its argument. Typically, the cylinders in a SIW are small when compared to the wavelength. This means that the Hankel functions associated to the higher order modes of (3) will return very high values when they are evaluated over the contour of the source cylinder. These extremely large values will be compensated by small values of the corresponding modal weights. Unfortunately, this fact will result in a very ill conditioned system of equations, since we will need a large number of modes to provide accurate results. In order to solve this problem, we will scale the modal weights and the diverging Hankel functions. Specifically, we will divide the diverging Hankel function by a large value and, at the same time, we will multiply the coefficient by the same number, in order to maintain an equivalent series. The coefficient chosen to correct the series will be the constant value equal to $H_n^{(2)}(kr_i)$. Then, if we define the new modal weight as $c_n^{(i)} = \hat{c}_n^{(i)} H_n^{(2)}(kr_i)$, (3) will become,

$$\vec{E}_i(\underline{c}_i, \vec{\rho}) = \sum_{n=-N_i}^{N_i} c_n^{(i)} \frac{H_n^{(2)}(k|\vec{\rho} - \vec{\rho}_i|)}{H_n^{(2)}(kr_i)} e^{\jmath n\phi} \hat{y} \tag{4}$$

Finally, to calculate the magnetic field generated by a cylindrical source, we will use the Maxwell's curl equations, that is

$$\vec{H}_i(\underline{c}_i, \vec{\rho}) = \frac{-1}{\jmath w\mu} \nabla \times \vec{E}_i(\underline{c}_i, \vec{\rho}) \tag{5}$$

so that,

$$H_{i\rho}(\underline{c}_i, \vec{\rho}) = \frac{-1}{w\mu\, R} \sum_{n=-N_i}^{N_i} c_n^{(i)}\, n\, \frac{H_n^{(2)}(kR)}{H_n^{(2)}(kr_i)} e^{\jmath n\phi} \tag{6}$$

$$H_{i\phi}(\underline{c}_i, \vec{\rho}) = \frac{k}{2\jmath w\mu} \sum_{n=-N_i}^{N_i} c_n^{(i)} \frac{H_{n+1}^{(2)}(kR) - H_{n-1}^{(2)}(kR)}{H_n^{(2)}(kr_i)} e^{\jmath n\phi} \tag{7}$$

where $R = |\vec{\rho} - \vec{\rho}_i|$.

Once we have elucidated how the field generated by the cylinders that form the SIW is going to be characterized, we will analyze how these expressions can be useful to improve the efficiency of the method of [1].

In [1], a general mode-matching and method of moments solver is particularized to analyze H-plane problems in rectangular waveguide. This particularization can be directly applied to the SIW case, thanks to its geometry. Therefore, if we apply the method of [1], keeping in mind that the cylinders can be modally characterized, the generic problem of Fig. 2 will produce the following system of equations,

$$\begin{pmatrix} \underline{\underline{Z}}_{11} & \underline{\underline{Z}}_{12} & \underline{\underline{Z}}_{13} \\ \underline{\underline{X}}_{21} & \underline{\underline{X}}_{22} & \underline{\underline{X}}_{23} \\ \underline{\underline{Z}}_{31} = 0 & \underline{\underline{Z}}_{32} & \underline{\underline{Z}}_{33} \end{pmatrix} \begin{pmatrix} \underline{b} \\ \underline{I}^a \\ \underline{C} \end{pmatrix} = \begin{pmatrix} \underline{E}_i \\ \underline{H}_i \\ 0 \end{pmatrix} \tag{8}$$

where $\underline{b}$ are the amplitudes of the guided modes reflected by the accessing ports, $\underline{I}^a$ are the weights of the currents used to expand the equivalent sources at the accessing ports, and $\underline{C}$ ($\underline{I}_c$ in [1]) exclusively contained the weights associated to

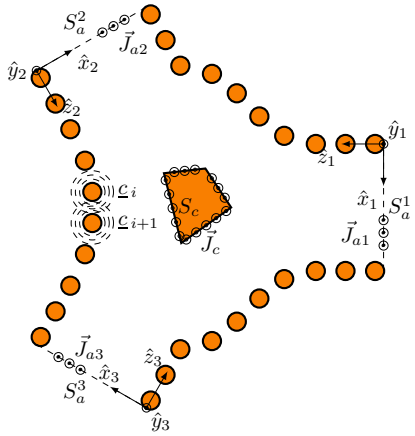

Fig. 2. Arbitrary SIW-based device.

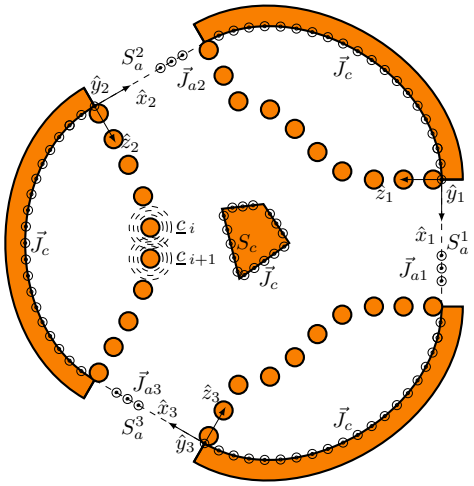

Fig. 3. Completely closed SIW-based arbitrary device.

the basis functions of the method of moments used to expand the unknown equivalent current. This current is induced over the conducting walls limiting the cavity and the contour of the scatterers inside this cavity by a known excitation. In the case we are studying here, the cylinders are modelled as modal sources instead of by means of an induced current. Therefore, in addition to the currents around the scatterers inside the SIW, we will have another set of unknowns, the modal weights necessary to calculate the scattered fields generated by the circular cylinders inside the SIW or limiting it. This means that $\underline{C}$ will have, in this case, two parts,

$$\underline{C} = \begin{pmatrix} \underline{I}_c \\ \underline{c} \end{pmatrix} \tag{9}$$

$\underline{I}_c$, which stores the weights used to reconstruct the current induced along the contour of the irregular scatterers, and $\underline{c}$, which stores the modal weights of the field scattered by the cylinders.

We have evaluated the contour conditions of the problem by applying point-matching. Pulse functions have been used to expand the current along the contour of the irregular scatterers and the ports, and the fields have been projected over Dirac's Delta functions uniformly distributed along the contours where the boundary conditions must be enforced. This means that, with the exception of the modal characterization of the circular scatterers, the rest of elements in (8) have the same meaning as in [1].

The first row of (8) contains a set of equations that enforces the tangential electric field continuity at the ports; the second row is a set of equations which enforces the tangential magnetic field continuity, again at the ports, and, finally, the last row enforces the tangential electric field at the contour of the circular and irregular scatterers to be zero.

III. Validity of the solution for an open cavity

The single current based equivalence of [1] is only possible if the region that is going to be analyzed is completely closed. This is not the case we are studying here, so the problem of Fig. 2 would be exactly characterized if, and only if, the problem is placed inside a closed cavity, as in Fig. 3. In this case, since the problem is exclusively excited through the ports, and assuming the SIW is well designed so that the field which escapes from it can be neglected, the field which reaches the limits of the cavity can be supposed to be zero. This means that there exist no currents along the limits of the auxiliary cavity that encloses the SIW and, therefore, it will not be necessary to consider them. Therefore, the problem of Fig. 2 will provide very accurate results, almost indistinguishable from the results of the problem of Fig. 3, with a noticeable lower computational cost. A similar discussion is used in [6] to justify the presence of equivalent currents only at the ports.

Moreover, the analysis of Fig. 3, although rigorous, is not realistic, because the extremely small field that escapes from the SIW, will reach the end of the substrate. To adequately characterize this situation, a 3D electromagnetic solver is necessary, since this phenomena cannot be modeled using a 2D approach. Fortunately, this effect is negligible, as we will see in the results section.

Due to all these reasons, we will analyze the SIW devices applying the discretization of Fig. 2, and we will see that it is perfectly valid since, in spite of the approximations, the results are highly accurate.

IV. Fast sweep

In order to obtain the frequency response of a given SIW device, it is necessary to solve the system of equations of (8) for a certain set of discrete frequencies close enough to appropriately describe the evolution of the response. This discrete frequency sweep is the most accurate, although the slowest as well.

Fortunately, there exist other alternatives that implement fast frequency sweeps. In order to perform a fast frequency sweep, maybe the most known technique is the asymptotic waveform evaluation (AWE) [14]–[18].

This technique is applied to solve a system of equations

$$\underline{\underline{A}}\,\underline{x} = \underline{q} \tag{10}$$

whose elements depend on a certain parameter, the frequency in our case, e.g.

$$\underline{\underline{A}}(f)\underline{x}(f) = \underline{q}(f) \tag{11}$$

In order to apply this method, we will suppose that all of the elements can be expressed in form of a Taylor's series. As a result, if we call

$$v^{(n)} = \frac{1}{n!}\frac{d^n(v(f))}{df^n} \tag{12}$$

with v equal to $\underline{\underline{A}}$, $\underline{x}$ or $\underline{q}$; and call $\Delta f = (f - f_0)$; the system of equations will become,

$$\begin{aligned}&\left(\underline{\underline{A}}(f_0) + \underline{\underline{A}}^{(1)}(f_0)\Delta f + \underline{\underline{A}}^{(2)}(f_0)\Delta f^2 + \ldots\right)\cdot\\ &\cdot\left(\underline{x}(f_0) + \underline{x}^{(1)}(f_0)\Delta f + \underline{x}^{(2)}(f_0)\Delta f^2 + \ldots\right) =\\ &= \underline{q}(f_0) + \underline{q}^{(1)}(f_0)\Delta f + \underline{q}^{(2)}(f_0)\Delta f^2 + \ldots\end{aligned} \tag{13}$$

After calculating the moments of $\underline{\underline{A}}$, i.e. $\underline{\underline{A}}^{(1)}, \underline{\underline{A}}^{(2)}, \ldots$, and $\underline{q}$; we can progressively calculate the moments of the unknown vector, $\underline{x}$. Specifically, [15], [17],

$$\underline{x}^{(n)} = \underline{\underline{A}}^{-1}(f_0)\left[\underline{q}^{(n)}(f_0) - \sum_{q=0}^{n}(1-\delta_{q0})\underline{\underline{A}}^{(q)}(f_0)\underline{x}^{(n-q)}\right] \tag{14}$$

where

$$\delta_{q0} = \begin{cases} 1, & \text{if } q = 0 \\ 0, & \text{if } q \neq 0 \end{cases} \tag{15}$$

Once we have the desired terms of the Taylor's series of the unknowns, we can use them to obtain a Padé approximation (polynomial quotient) of the elements of $\underline{x}$, since the Padé approximation is more appropriate to characterize the frequency evolution of the scattering parameters of a passive device. The calculation of the Padé approximation from the Taylor's series can be found in [16]–[18].

The only difficulty in the application of AWE is to find a relatively easy and costless procedure to calculate the moments of $\underline{\underline{A}}$ and $\underline{q}$. In our case, $\underline{\underline{A}}$, is the matrix of coefficients of (8) and $\underline{q}$ is the excitation. Fortunately, $\underline{q}$ can be extracted from the first columns of $\underline{\underline{A}}$ (see [1]). Therefore, to apply AWE to our problem, we only need to find the moments of the matrix $\underline{\underline{A}}$.

In order to calculate the moments of $\underline{\underline{A}}$ we need to calculate the successive partial derivatives of its elements with respect to the frequency. The elements, which belong to the second and third columns of $\underline{\underline{A}}$, are Hankel functions, so it is possible to calculate its kth-order derivative analytically [23]–[25].

Unfortunately, these Hankel functions are multiplied by the frequency or appear in the form of a quotient of Hankel functions (see (4), (6) and (7)). This means that the difficulty to calculate these derivatives increases notably and implies a very high computational cost, since they require the evaluation of several Hankel functions.

However, the calculation of the analytical derivatives is not necessary, since we have observed that the frequency variation of those elements can be extremely well approximated using the following expression,

$$z_{mn}(f) = \left[G_{mn} + C_{mn}(f - f_0)\right]e^{\jmath(H_{mn}+D_{mn}(f-f_0))} \tag{16}$$

where

$$G_{mn} = |z_{mn}(f_0)| \tag{17}$$

$$C_{mn} = \left.\frac{d[|z_{mn}(f)|]}{df}\right|_{f=f_0} \tag{18}$$

$$H_{mn} = \angle(z_{mn}(f_0)) \tag{19}$$

$$D_{mn} = \left.\frac{d[\angle(z_{mn}(f))]}{df}\right|_{f=f_0} \tag{20}$$

The moments obtained using this approximation are very similar to those obtained with the analytical derivatives. Since the approximation requires less computational effort, we have preferred it to the analytical results for the calculation of the moments.

Moreover, to confirm the validity of the approximation of (16), we have compared the reconstruction of the matrix of coefficients from its moments to the direct calculation of the matrix for several frequencies. The reconstructed and the directly computed matrices are very similar. Definitely, this fact sustains the goodness of the approximation of (16).

If we use this approximation, the first derivative with respect to the frequency of the elements of the second and third columns of $\underline{\underline{A}}$ can be computed as,

$$\frac{d[z_{mn}(f)]}{df} = \left[G_{mn}^{(1)} + C_{mn}^{(1)}(f - f_0))\right]e^{\jmath(H_{mn}+D_{mn}(f-f_0))} \tag{21}$$

where

$$G_{mn}^{(1)} = C_{mn} + \jmath D_{mn}G_{mn} \tag{22}$$

$$C_{mn}^{(1)} = \jmath D_{mn}C_{mn} \tag{23}$$

The first derivative has the same structure as the original function. Therefore, the expression for the n-th derivative will be

$$\frac{d^n[z_{mn}(f)]}{df^n} = \left[G_{mn}^{(n)} + C_{mn}^{(n)}(f - f_0))\right]e^{\jmath(H_{mn}+D_{mn}(f-f_0))} \tag{24}$$

where

$$G_{mn}^{(n)} = C_{mn}^{(n-1)} + \jmath D_{mn}G_{mn}^{(n-1)} \tag{25}$$

$$C_{mn}^{(n)} = \jmath D_{mn}C_{mn}^{(n-1)} \tag{26}$$

The moments we are looking for are these derivatives evaluated at f_0 and divided by a certain factorial factor, i.e.

$$z_{mn}^{(n)} = \frac{1}{n!}G_{mn}^{(n)}e^{\jmath H_{mn}} \tag{27}$$

We have applied this approximation to obtain the moments of the elements of the second and third columns of $\underline{\underline{A}}$. However, we have not found a good enough frequency approximation for the elements of the first column nor an analytical expression for their derivatives. This is the reason why we have computed the moments of these elements numerically.

AWE can be applied to quickly calculate the frequency response of a passive narrowband SIW device. For wideband devices complex frequency hopping [19], [20], can be used.

The complex frequency hopping is simply a successive application of AWE. The desired bandwidth is divided in several pieces and AWE is applied independently to every single piece.

The only difficulty of complex frequency hopping is to find the appropriate division of the bandwidth. For its simplicity, we have applied the algorithm in Section V, subsection A of [26] to determine such frequency intervals.

V. Losses

In order to characterize the losses in the conductors, we apply the concept of square impedance, Z_S, since it allows the application of the well-known Leontovich's contour condition [27]

$$\vec{E}_t - Z_S \vec{H}_t = 0 \tag{28}$$

where $Z_S = \sqrt{(w\mu)/(2\sigma)}(1+\jmath)$ is the square impedance of the conductor and σ its conductivity; $\vec{E}_t$ and $\vec{H}_t$ are the fields, electric and magnetic respectively, tangential to its external surface.

Since the boundary condition is now different, it is necessary to modify the third row of (8). Two new matrices, $\underline{\underline{X}}_{32}$ and $\underline{\underline{X}}_{33}$, have to be defined. $\underline{\underline{X}}_{32}$ is a matrix, which multiplied by the currents at the ports, gives the discretization of the magnetic field, generated by those currents, tangential to the irregular or circular metallic scatterers. On the other hand, $\underline{\underline{X}}_{33}$ is a matrix, which multiplied by the modal weights of the via holes and the currents of the irregular metallic scatterers, gives the magnetic field, generated by those sources, tangential to the metallic scatterers.

By using these two new matrices, the system of (8) becomes

$$\begin{pmatrix} \underline{\underline{Z}}_{11} & \underline{\underline{Z}}_{12} & \underline{\underline{Z}}_{13} \\ \underline{\underline{X}}_{21} & \underline{\underline{X}}_{22} & \underline{\underline{X}}_{23} \\ \underline{\underline{Z}}_{31}=0 & \underline{\underline{T}}_{32} & \underline{\underline{T}}_{33} \end{pmatrix} \begin{pmatrix} \underline{b} \\ \underline{I}^a \\ \underline{C} \end{pmatrix} = \begin{pmatrix} \underline{E}_i \\ \underline{H}_i \\ 0 \end{pmatrix} \tag{29}$$

with $\underline{\underline{T}}_{32} = \underline{\underline{Z}}_{32} - Z_S \underline{\underline{X}}_{32}$ y $\underline{\underline{T}}_{33} = \underline{\underline{Z}}_{33} - Z_S \underline{\underline{X}}_{33}$

Simultaneously, we can also characterize the dielectric losses if we calculate the elements of (29) using the complex permittivity, $\epsilon^{(loss)} = \epsilon_0 \epsilon_r (1 - \jmath \tan\delta)$, where $\tan\delta$ is the loss tangent of the dielectric.

VI. Results

We have tested the efficiency and accuracy of our method by analyzing the four coupled cavity filter and the hybrid ring of Fig. 4. This hybrid ring is a design of [6], which has been adapted to the substrate we have used to fabricate these devices, a Rogers RO4003(tm) dielectric substrate of 1.525 mm height with 35 μm copper metalization layers, and a dielectric constant of 3.55. The dimensions of the filter and the ring can be seen in Tabs. I and II, respectively.

TABLE I
Dimensions for the filter of Fig. 4(a).

$L_1 = 8.515$ mm	$L_2 = 9.165$ mm	$w = 12.8$ mm
$w_1 = 5.516$ mm	$w_2 = 3.506$ mm	$w_c = 3.29$ mm
$s = 1.3$ mm	$s_i = 1.2$ mm	$d = 0.8$ mm

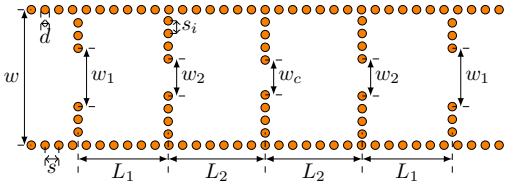

(a) Filter

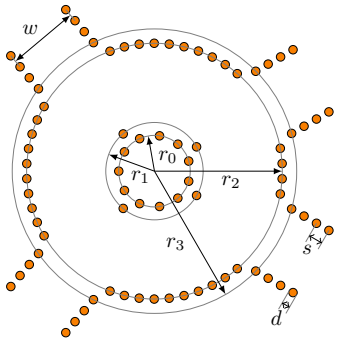

(b) Hybrid ring

Fig. 4. Layout of the filter with four coupled cavities and the hybrid ring.

TABLE II
Dimensions for the hybrid ring of Fig. 4(b).

$r_0 = 3.373$ mm	$r_1 = 4.594$ mm	$r_2 = 12.086$ mm
$r_3 = 13.442$ mm	$w = 6.78$ mm	$s = 1.356$ mm
$d = 0.8$ mm		

Fig. 5 shows the comparison between the results obtained by applying the technique of this paper and the results provided by the commercial software Ansoft HFSS for the filter of Fig. 4(a). We have solved the device with (Fig. 5(b)) and without (Fig. 5(a)) considering the dielectric and metallic losses. It can be observed that there is a complete agreement between the discrete sweep response and the fast sweep responses, both with AWE and CFH.

The technique presented in this paper can only be applied to solve the SIW problem, since it is essentially a 2D approach. In order to obtain the solution of the same problem fed through microstrip lines, a 3D simulator will be necessary. The geometry of the adaptation taper, which would allow us to feed the problem through a microstrip, does not depend on the specific SIW device analyzed. So the taper can be designed and solved apart. Therefore, we can still use the bidimensional approach to design and analyze these SIW devices. First, we have designed and solved the taper by means of a commercial 3D solver (HFSS), and we have computed its generalized scattering matrix. After this, we have analyzed the device by using HFSS and the technique presented in this paper, and we have computed its generalized scattering matrix as well. Finally, by applying the well-known method of the generalized scattering matrix [28], we have cascaded the different matrices to obtain the response of the filter with the tapers.

Fig. 7 shows the results of the filter of Fig. 6(b). The dimensions and geometry of the taper can be seen at Fig. 6(a). The results of the hybrid technique are compared with the HFSS analysis of the filter by pieces; with the full HFSS

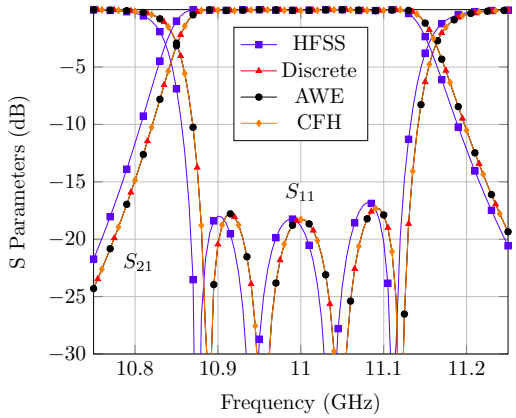

(a) Without losses

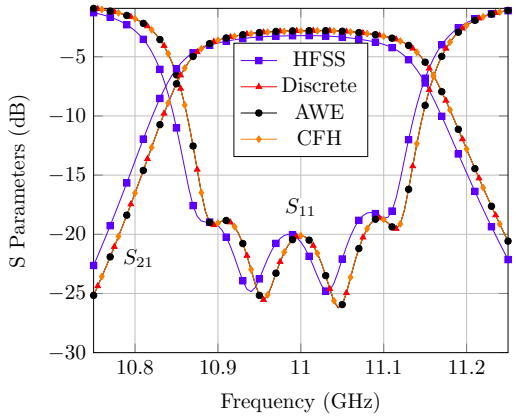

(b) With losses (RO4003(tm) substrate: $\tan\delta = 0,0027$, $\sigma = 5,813 \cdot 10^7$)

Fig. 5. Results for the filter of Fig. 4(a). Fast and discrete sweep, with (RO4003(tm) and copper) and without losses.

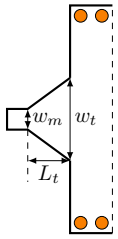

$w_m = 3.65$ mm
$w_t = 5.1$ mm
$L_t = 3$ mm

(a) Taper layout

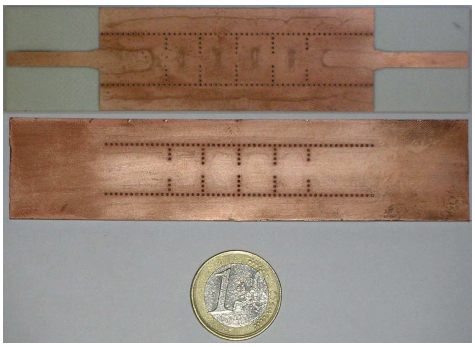

(b) Real filter

Fig. 6. Layout of the microstrip-to-SIW transition and fabricated prototype.

analysis of the filter (considering the tapers and the SIW at the same time); and with experimental results.

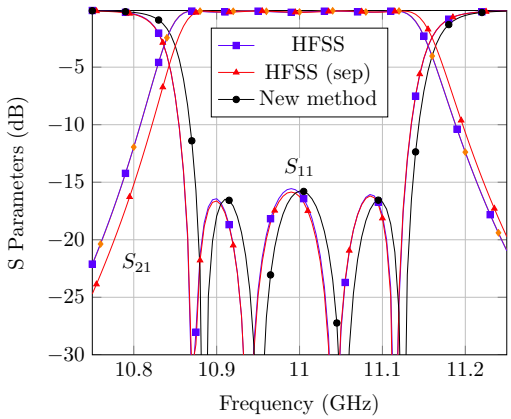

(a) Without losses

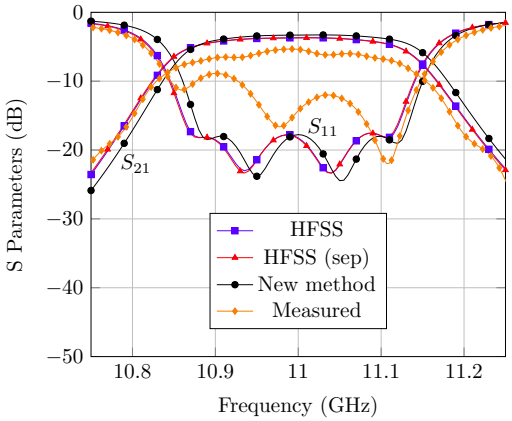

(b) With losses (RO4003(tm) substrate: $\tan\delta = 0,0027$, $\sigma = 5,813 \cdot 10^7$)

Fig. 7. Results for the filter of Fig. 6 with (RO4003(tm) and copper) and without losses. The results of the hybrid technique (circles) are compared with the HFSS analysis of the filter by pieces (triangles); the HFSS analysis of the filter considering the tapers and the SIW at the same time (squares); and measurements (diamonds).

Finally, in Tab. III, we have tabulated the temporal costs associated to the analysis of the SIW part of the problem (the filter without tapers). We exclusively compare the cost of this part because, in a design process, the taper needs to be analyzed only once, while the SIW part has to be progressively tuned and, therefore, solved multiple times.

TABLE III
COST COMPARISON.

	HFSS		New method		
	Discrete	Fast	Discrete	AWE	CFH
With losses	11821 s	1756 s	387 s	15 s	30 s
Without losses	15415 s	1721 s	218 s	10 s	20 s

The technique proposed here improves notably the efficiency provided by the commercial software HFSS, which we have used as reference. This improvement can be noticed not only in the case of the discrete sweep, but also in the fast sweep.

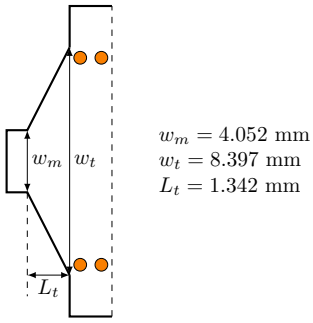

(a) Taper layout

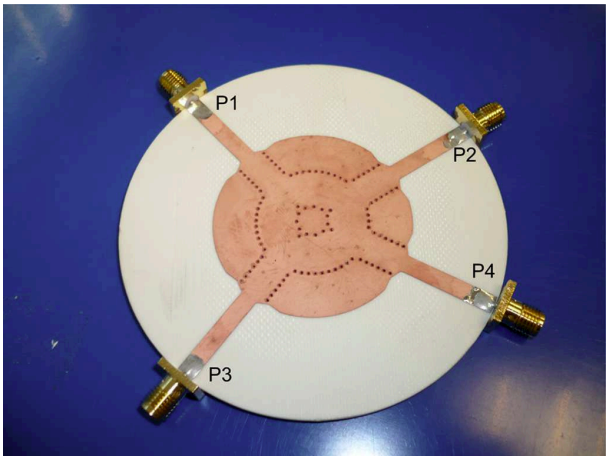

(b) Real hybrid

Fig. 8. Fabricated prototype of the hybrid ring of Fig. 4(b) and taper dimensions.

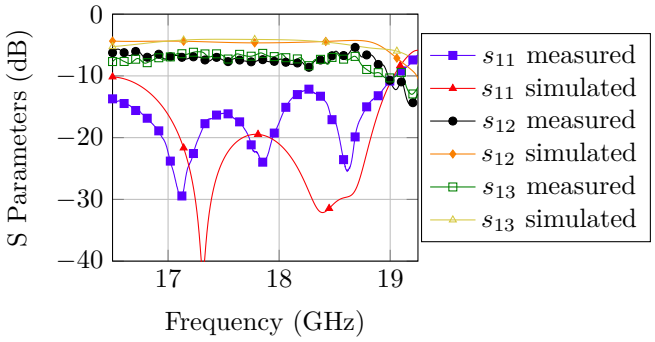

(a) Parameters S_{11}, S_{12} and S_{13}

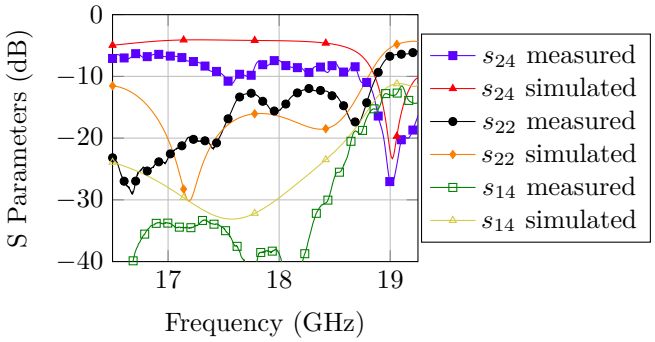

(b) Parameters S_{24}, S_{22} and S_{14}

Fig. 9. Measured vs. simulated results for the hybrid of Fig. 8(b).

As we advanced at the beginning of the section, we have also tested the method using a multiport device, specifically, the hybrid ring of Fig. 8(b). As we have done before with the filter, the generalized scattering matrix of the taper of Fig. 8(a) has been computed using HFSS. In this case, the full response of the device has been calculated by cascading five generalized scattering matrices [28], four tapers and the hybrid, which has been solved using the technique presented in this paper. The computational cost for this same device in [6] was 12 seconds per frequency point with a 3.6 GHz processor. The new method requires 2.2 seconds per frequency point with discrete sweep and an Intel Core 2 Duo processor at 2.8 GHz and 4 Gb of RAM memory. For a response with 60 points, 720 seconds are required in [6] (discrete sweep), 1362 seconds with HFSS (fast sweep), and 10.72 seconds with the new method and using the AWE fast sweep.

Figs. 9(a) and 9(b) show the comparison between the simulation and the measured data. The differences that can be observed in the results are due to the fact that the simulation does not consider the losses produced by the coaxial-to-microstrip connectors we have used to excite the microstrip ports (see Fig. 8(b)). The results of the filter show the same discordance, which is due to the same fact.

VII. Conclusion

We have adapted the general hybrid method of moments and mode-matching technique of [1] to the analysis of passive SIW devices. In addition, we have applied the modal characterization of the SIW via holes of [6] to the technique presented in this paper, and proposed a correction to the modal weights in order to improve the conditioning of the resulting system of equations. Finally, we have also proposed an original and very accurate approximation to characterize the frequency dependence of the elements of the matrix of coefficients of the new method. This approximation has allowed us to successfully and efficiently apply two different fast sweep strategies, asymptotic waveform evaluation and complex frequency hopping.

Because of this, we have formulated an analysis technique that is highly competitive in terms of efficiency and accuracy. This technique can be used to very efficiently analyze passive SIW devices as one can see in Tab. III, where the solution times are compared to HFSS. In addition, the results are also very accurate. Figs. 5, 7, and 9 show the results provided by the technique presented in this paper, the results of HFSS, and experimental measures. A great coincidence is observed when these different responses are compared.

References

[1] A. Belenguer, H. Esteban, V. E. Boria, C. Bachiller, and J. V. Morro, "Hybrid mode matching and method of moments method for the full-wave analysis of arbitrarily shaped structures fed through canonical waveguides using only electric currents," *IEEE Transactions on Microwave Theory and Techniques*, vol. 58, no. 3, pp. 537–544, Mar. 2010.

[2] A. Wexler, "Solution of waveguide discontinuities by modal analysis," *IEEE Trans. Microwave Theory Tech.*, vol. 15, no. 9, pp. 508–517, Sep. 1967.

[3] R. F. Harrington, *Field Computation by Moment Methods*, ser. IEEE Press / OUP Series on Electromagnetic Wave Theory. IEEE Press / OUP, 1993.

[4] S. A. Schelkunoff, "Some equivalence theorems of electromagnetics and their application to radiation problems," *Bell System Tech. Journal*, vol. 15, pp. 92–112, 1936.
[5] C. A. Balanis, *Antenna theory : analysis and design*, 2nd ed. NY: John Wiley & Sons, Inc., 1997.
[6] X. Wu and A. Kishk, "Hybrid of method of moments and cylindrical eigenfunction expansion to study substrate integrated waveguide circuits," *IEEE Transactions on Microwave Theory and Techniques*, vol. 56, no. 10, pp. 2270 –2276, Oct. 2008.
[7] D. Deslandes and K. Wu, "Integrated microstrip and rectangular waveguide in planar form," *IEEE Microwave and Wireless Components Letters*, vol. 11, no. 2, pp. 68–70, Feb. 2001.
[8] ——, "Single-substrate integration technique of planar circuits and waveguide filters," *IEEE Transactions on Microwave Theory and Techniques*, vol. 51, no. 2, pp. 593–596, Feb. 2003.
[9] ——, "Accurate modeling, wave mechanisms, and design considerations of a substrate integrated waveguide," *IEEE Transactions on Microwave Theory and Techniques*, vol. 54, no. 6, pp. 2516–2526, Jun. 2006.
[10] M. Bozzi, L. Perregrini, and K. Wu, "Direct Determination of Multimode Equivalent Circuit Models for Discontinuities in Substrate Integrated Waveguide Technology," in *Microwave Symposium Digest, 2006. IEEE MTT-S International*. IEEE, 2007, pp. 68–71.
[11] ——, "Modeling of losses in substrate integrated waveguide by Boundary Integral-Resonant Mode Expansion method," in *Microwave Symposium Digest, 2008 IEEE MTT-S International*. IEEE, 2008, pp. 515–518.
[12] F. Mira, A. San Blas, V. Boria, and B. Gimeno, "Fast and accurate analysis and design of substrate integrated waveguide (SIW) filters," in *Microwave Conference, 2007. European*. IEEE, 2007, pp. 170–173.
[13] F. Mira, A. San Blas, S. Cogollos, V. Boria, and B. Gimeno, "Computer-aided design of substrate integrated waveguide filters for microwave and millimeter-wave applications," in *Microwave Conference, 2009. EuMC 2009. European*. IEEE, 2009, pp. 425–428.
[14] L. T. Pillage and R. A. Rohrer, "Asymptotic waveform evaluation for timing analysis," *IEEE Transactions on Computer-Aided Design of Integrated Circuits and Systems*, vol. 9, no. 4, pp. 352 –366, Apr. 1990.
[15] C. R. Cockrell and F. B. Beck, "Asymptotic waveform evaluation (AWE) technique for frequency domain electromagnetic analysis," NASA Technical Memorandum 110292, 1996.
[16] Y. E. Erdemli, C. J. Reddy, and J. L. Volakis, "AWE techniques in frequency domain electromagnetics," NASA Langley Research Center, 030601-12-T. http://hdl.handle.net/2027.42/21454, 1997.
[17] C. J. Reddy, M. D. Deshpande, C. R. Cockrell, and F. B. Beck, "Fast RCS computation over a frequency band using method of moments in conjunction with asymptotic waveform evaluation technique," *IEEE Transactions on Antennas and Propagation*, vol. 46, no. 8, pp. 1229–1233, 1998.
[18] Y. E. Erdemli, C. J. Reddy, and J. L. Volakis, "AWE technique in frequency domain electromagnetics," *Journal of Electromagnetic Waves and Applications*, vol. 13, no. 3, pp. 359–378, 1999.
[19] E. Chiprout, H. Heeb, M. S. Nakhla, and A. E. Ruehli, "Simulating 3-D retarded interconnect models using complex frequency hopping (CFH)," in *IEEE/ACM International Conference on Computer-Aided Design, 1993. ICCAD-93. Digest of Technical Papers, 1993*, Nov. 1993, pp. 66 –72.
[20] E. Chiprout and M. S. Nakhla, "Analysis of interconnect networks using complex frequency hopping (CFH)," *IEEE Transactions on Computer-Aided Design of Integrated Circuits and Systems*, vol. 14, no. 2, pp. 186 –200, Feb. 1995.
[21] H. Esteban, S. Cogollos, V. Boria, A. Blas, and M. Ferrando, "A new hybrid mode-matching/numerical method for the analysis of arbitrarily shaped inductive obstacles and discontinuities in rectangular waveguides," *Microwave Theory and Techniques, IEEE Transactions on*, vol. 50, no. 4, pp. 1219–1224, 2002.
[22] P. Li, A. Adams, Y. Leviatan, and J. Perini, "Multiple-post inductive obstacles in rectangular waveguide," *Microwave Theory and Techniques, IEEE Transactions on*, vol. 32, no. 4, pp. 365–373, 1984.
[23] M. Abramowitz and I. A. Stegun, *Handbook or Mathematical Functions*. NY: Dover Pubns., 1965.
[24] "Bessel-type functions," From MathWorld-A Wolfram Web Resource, http://functions.wolfram.com/Bessel-TypeFunctions/.
[25] R. Slevinsky and H. Safouhi, "New formulae for higher order derivatives and applications," *Journal of Computational and Applied Mathematics*, vol. 233, no. 2, pp. 405–419, 2009.
[26] R. Achar, M. S. Nakhla, and Q.-J. Zhang, "Full-wave analysis of high-speed interconnects using complex frequency hopping," *IEEE Transactions on Computer-Aided Design of Integrated Circuits and Systems*, vol. 17, no. 10, pp. 997 –1016, Oct. 1998.
[27] T. B. A. Senior and J. L. Volakis, *Aproximate boundary conditions in electromagnetics*. LON: Institution of Electrical Engineers, 1995.
[28] P. Overfelt and D. White, "Alternate forms of the generalized composite scattering matrix," *IEEE Transactions on Microwave Theory and Techniques*, vol. 37, no. 8, pp. 1267–1268, AGO 1989.

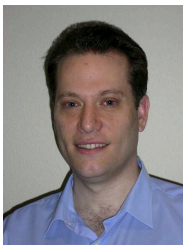

Angel Belenguer (M'04) received the Telecommunication Engineering and Ph.D. degrees from the Universidad Politécnica de Valencia, Spain, in 2000 and 2009, respectively. He joined the Universidad de Castilla-La Mancha in 2000, where he is now Profesor Titular de Escuela Universitaria in the Departamento de Ingeniería Eléctrica, Electrónica, Automática y Comunicaciones. His research interests include methods in the frequency domain for the full-wave analysis of open-space and guided multiple scattering problems, specifically the improvement or acceleration of these methods using several strategies: hybridization of two or more different methods, the use of specific basis, and the application of accelerated solvers or solving strategies to new problems or structures.

Héctor Esteban (S'93−M'99) received a degree in telecommunications engineering from the Universidad Politécnica de Valencia (UPV), Spain, in 1996, and a Ph.D. degree in 2002. He worked with the Joint Research Centre, European Commission, Ispra, Italy. In 1997, he was with the European Topic Centre on Soil (European Environment Agency). He rejoined the UPV in 1998. His research interests include methods for the full- wave analysis of open-space and guided multiple scattering problems, CAD design of microwave devices, electromagnetic characterization of dielectric and magnetic bodies, and the acceleration of electromagnetic analysis methods using the wavelets and the FMM.

Elena Diaz (S'07) has recently received the Telecommunication Engineering degree from the Universidad Politécnica de Valencia (UPV), Spain, in July 2010, and is about to begin her work toward the Ph.D. degree at UPV. She won a Collaboration Fellowship at the Communications Department of UPV in 2009, and has recently done an internship at AURORASAT Company. Her research interest is currently focused in the development of efficient methods for the analysis and design of substrate integrated waveguide devices

Carmen Bachiller (GSM'05) received her degree in communication engineering from the Universidad Politécnica de Valencia in 1996. She worked from 1997 to 2001 in the ETRA I+D company as a project engineer in research and development on automatic traffic control, public transport management and public information systems using telecommunication technology. In 2001 she joined the Communication Department of the Universidad Politécnica de Valencia as an assistant lecturer. She is teaching signal and systems theory and microwaves. She has participated in several teaching innovation projects. She is now working in her Ph.D. thesis on electromagnetism and radio frequency circuits.

Joaquín Cascón was born in Cuenca, Spain, in 1966. He received his degree in Telecommunications engineering from the Universidad Politécnica de Madrid (UPM), Spain, in 1991, and PhD from the Universidad Politécnica de Valencia, (UPV), Spain, in 1999. From 1991 to 1999 he was with the Optical Communication Group, UPV, where he worked in Optical Communications. In 1999 he joined the Departamento de Ingeniería Eléctrica, Electrónica, Automática y Comunicaciones, Universidad de Castilla-La Mancha (Spain), he is now Catedrático de Escuela Universitaria . His current research interest include EM metamaterials, antennas, tunable structures and their applications in microwave and millimeter-wave technologies.

Vicente E. Boria (S'91−A'99−SM'02) received the *Ingeniero de Telecomunicacin* and the *Doctor Ingeniero de Telecomunicacin* degrees from the Universidad Politécnica de Valencia, Spain, in 1993 and 1997. In 1993 he joined the Universidad Politécnica de Valencia where he is Full Professor since 2003. In 1995 and 1996 he was held a Spanish Trainee position with the European Space research and Technology Centre (ESTEC)-European Space Agency (ESA). He has served on the Editorial Boards of the IEEE Transactions on Microwave Theory and Techniques. His current research interests include numerical methods for the analysis of waveguide and scattering structures, automated design of waveguide components, radiating systems, measurement techniques, and power effects in passive waveguide systems.